Peer reviewed version

License (if available):
Unspecified

Link to published version (if available):
10.1021/acs.chemrestox.5b00514

Link to publication record in Explore Bristol Research
PDF-document

University of Bristol - Explore Bristol Research
General rights

Quantum mechanics/molecular mechanics modeling of drug metabolism: Mexiletine N-hydroxylation by cytochrome P450 1A2

Richard Lonsdale,[†,¶] Rachel M. Fort,[†] Patrik Rydberg,[‡] Jeremy N. Harvey,[†,§] and Adrian J. Mulholland[*,†]

†Centre for Computational Chemistry, School of Chemistry, University of Bristol, Cantock's Close, Bristol, BS8 1TS, UK

‡Department of Drug Design and Pharmacology, Faculty of Health and Medical Sciences, University of Copenhagen, Universitetsparken 2, DK-2100, Copenhagen, Denmark

¶Current address: Oncology iMed, AstraZeneca, Cambridge CB4 0FZ, UK

§Current address: Quantum Chemistry and Physical Chemistry Section, Department of Chemistry, University of Leuven (KU Leuven), Celestijnenlaan 200F - box 2404, Leuven, Belgium

E-mail: adrian.mulholland@bristol.ac.uk

Phone: +44-(0)117-928-9097. Fax: +44-(0)117-925-0612

Running header

QM/MM modeling of Mexiletine N-hydroxylation by CYP1A2

Abstract

The mechanism of cytochrome P450(CYP)-catalyzed hydroxylation of primary amines is currently unclear, and is relevant to drug metabolism. Previous small model calcula-

tions have suggested two possible mechanisms: direct N-oxidation and H-abstraction/rebound. We have modeled the N-hydroxylation of (R)-mexiletine in CYP1A2 with hybrid quantum mechanics/molecular mechanics (QM/MM) methods, providing a more detailed and realistic model. Multiple reaction barriers have been calculated at the QM(B3LYP-D)/MM(CHARMM27) level for the direct N-oxidation and H-abstraction/rebound mechanisms. Our calculated barriers indicate that the direct N-oxidation mechanism is preferred and proceeds via the doublet spin state of Compound I. Molecular dynamics simulations indicate that the presence of an ordered water molecule in the active site assists in the binding of mexiletine in the active site, but is not a prerequisite for reaction via either mechanism. Several active site residues play a role in the binding of mexiletine in the active site, including Thr124 and Phe226. This work reveals key details in the N-hydroxylation of mexiletine and further demonstrates that mechanistic studies using QM/MM methods are useful for understanding drug metabolism.

Introduction

The cytochromes P450 (CYPs) play an important role in drug metabolism:[1,2] indeed, over 70 % of all drugs are metabolized by one of four CYPs (3A4, 2C9, 2D6, 1A2) at some stage in their metabolic pathway.[3,4] The metabolism of drugs by CYPs can lead to adverse reactions,[5] and hence predictions of CYP metabolism will help in the design of safer medicines. To enable accurate predictions, an understanding of the reaction mechanisms is important, as the models used to estimate reactivities depend on this.[6] The mechanisms of CYPs are difficult to study experimentally, due to their high activity, and the instability of their active species, Compound I (Cpd I).[7,8] Several mechanistic studies have been performed using quantum mechanics/molecular mechanics (QM/MM) for CYP isoforms.[9,10] However, these studies have been mostly performed on model substrates, and relatively few pharmaceutical compounds have so far been modeled.[11–16]

CYP1A2 is involved in drug metabolism, and is found in the endoplasmic reticulum of

liver cells, constituting 12% of the CYPs in the liver.[1] Substrates of CYP1A2 are typically hydrophobic, with high logP values,[17,18] and include caffeine, clozapine, theophylline and mexiletine.[2] CYP1A2 also metabolizes the endogenous substrates estrone and 17-estradiol.[19] Mexiletine (**1**) is used to treat ventricular dysrhythmias,[20,21] and is administered in a racemic mixture of R- and S-enantiomers, with the R-enantiomer being slightly more potent.[22] Mexiletine has a narrow therapeutic index[23,24] and is metabolized by several CYPs.[25] Together with CYP2E1 and CYP2B6, CYP1A2 is involved in the N-hydroxylation of mexiletine to form N-hydroxmexiletine (**2**, Scheme 1).[26] The hydroxylation of N-hydroxmexiletine occurs ten times faster in CYP1A2 for the R-, compared to the S-enantiomer. Hydroxymethylmexiletine (**3**) and p-hydroxymexiletine (**4**) are also formed during metabolism of mexiletine by CYP1A2.[27] The latter two metabolites, together with m-hydroxymexiletine (**5**) are also formed due to metabolism by CYP2D6.[25,28] CYP2D6 is known to react with substrates which contain a basic protonated amine group at a distance of ~ 7 Å from the site of oxidation,[29] due to interactions with Glu216 and Asp301, which line the active site and are believed to be important for substrate binding. CYP1A2 has a known preference for hydrophobic substrates[17,18] and therefore it is unlikely that the amine group of mexiletine will be protonated in the active site of CYP1A2. The NH_2 nitrogen of mexiletine is 5-7 Å from the known sites of oxidation in CYP2D6, and may explain why N-hydroxylation is not observed for oxidation of mexiletine by CYP2D6.

It is important to understand the mechanism behind the formation of hydroxylamines, such as **2**, because some related compounds have been found to be toxic.[30] Three possible mechanisms have been proposed for N-hydroxylation of primary amines by CYPs:[31] H-abstraction followed by rebound, direct N-oxidation followed by rearrangement of the N-oxide to the hydroxylamine, and direct O-insertion to the N-H bond (Scheme 2). The H-abstraction/rebound pathway is the widely accepted mechanism for the hydroxylation of aliphatic carbon atoms,[32] and involves the abstraction of a hydrogen atom from the substrate by Cpd I, forming a radical and a hydroxy-iron complex; the subsequent step
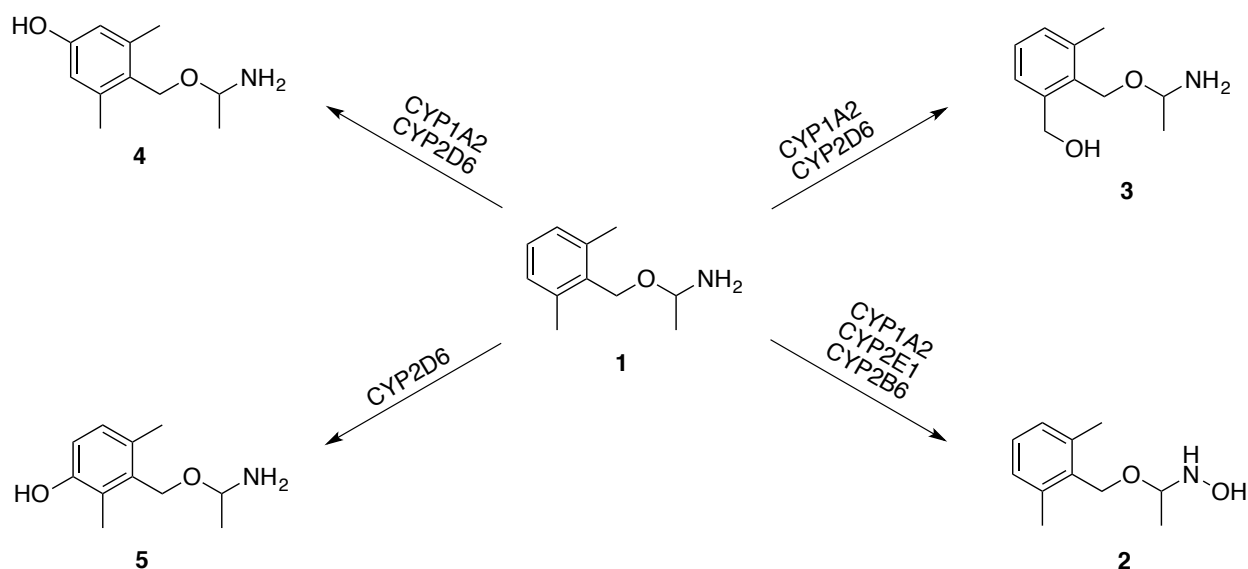
Scheme 1: Cytochrome P450 mediated metabolism of mexiletine (**1**) in humans.[25–28]

is the 'rebound' step, whereby the substrate-oxygen bond is formed. This mechanism is supported by experimental measurement of kinetic isotope effects,[7] which to our knowledge have not been measured for the hydroxylation of amines by CYPs.

The oxidation of primary and secondary amines by Cpd I has previously been studied in small models by DFT calculations.[33,34] The direct insertion of Cpd I ferryl oxygen into the N-H bond of propan-2-amine was found to be energetically unfavorable, and can thus be discounted as a mechanism for the *N*-hydroxylation of primary amines.[33] The calculated energy barriers to the remaining mechanisms were similar to each other, the relative ordering was found to depend on the value of the dielectric when a polarized continuum model was applied (direct oxygen insertion was favored in water, H-abstraction/rebound was favored in protein). A more recent study of propan-2-amine hydroxylation by the same group[34] in which the DFT calculations included an empirical dispersion correction, found the H-abstraction/rebound pathway to be preferred by around 2 kcal/mol. The hydroxylation of primary aromatic amines has also been recently studied.[35] Several proposed mechanisms were studied using aniline and *p*-substituted derivatives. The authors concluded that the most energetically feasible mechanism corresponded to hydrogen abstraction, followed by
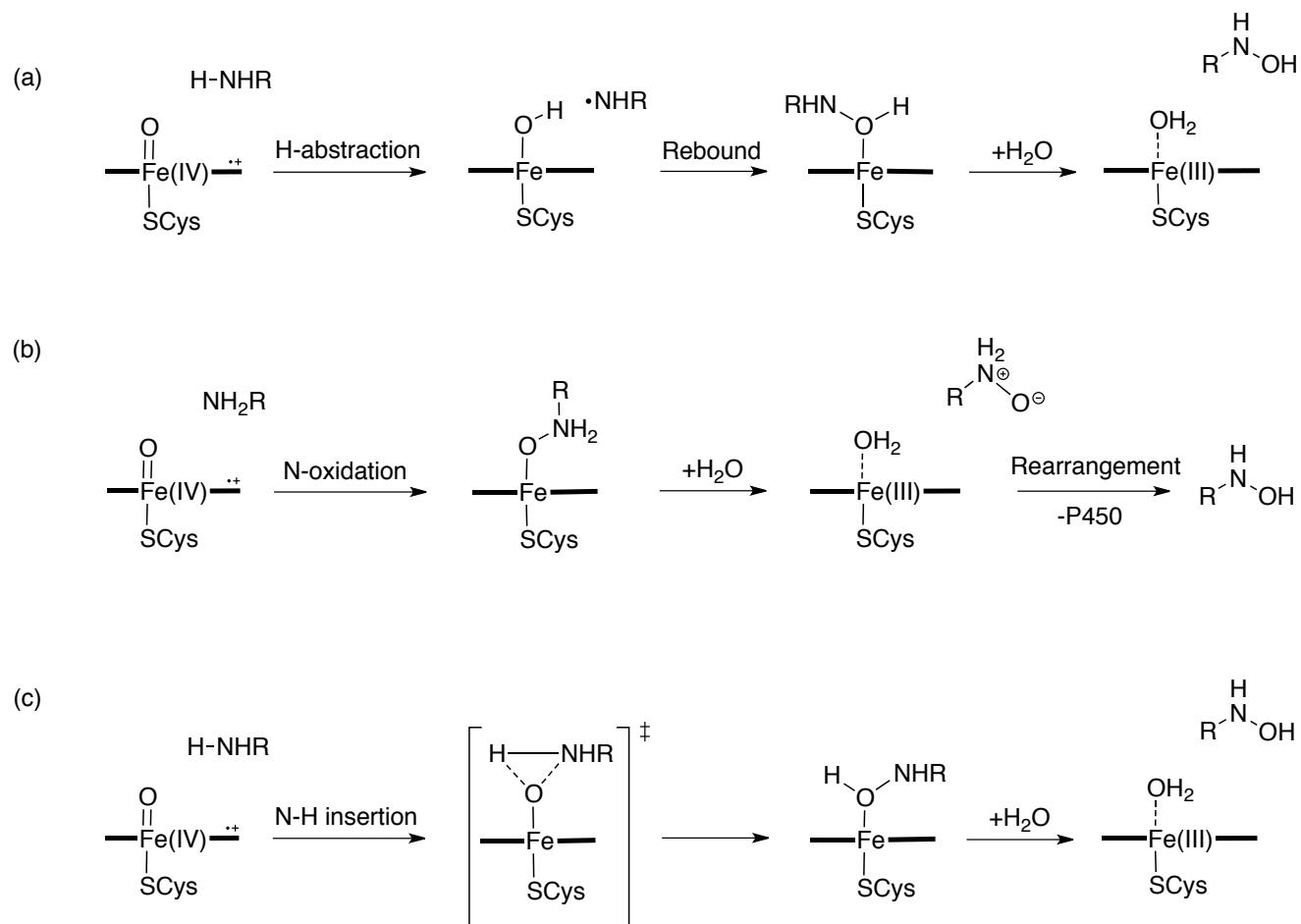
Scheme 2: Proposed mechanisms[31] for hydroxylation of primary amine RNH_2 by Compound I: (a) H-abstraction followed by rebound; (b) direct N-oxidation followed by rearrangement; (c) direct insertion into N-H bond. Previous calculations[33] indicate mechanism (c) is not energetically feasible and hence only mechanisms (a) and (b) are considered in this study.

rebound. The barrier to hydrogen abstraction was calculated to be 3.7 and 3.9 kcal/mol for the doublet and quartet spin states of Cpd I, respectively (at the UB3LYP/LACVP-6-31+G(d,p) level). The possible involvement of electron transfer mechanisms in the oxidation of amines by CYPs has also been investigated for both aniline[35] and tertiary amines,[36] and was found to be unlikely in both cases.

In this study, the mechanism of primary amine hydroxylation by CYPs has been investigated using a large and detailed CYP1A2:mexiletine complex, constructed using docking and molecular dynamics simulations. Different binding conformations of mexiletine were selected and used to calculate multiple QM(B3LYP-D)/MM(CHARMM27) reaction profiles for the proposed H-abstraction/rebound and direct N-oxidation mechanisms. Our results suggest that both reaction pathways may contribute towards the reactivity of Cpd I with primary amines, and we identify important binding interactions between the substrate and active site of CYP1A2.

Computational details

The initial structure of the enzyme used in the present study was built from a crystal structure of CYP1A2 (PDB code: 2HI4).[37] Docking and molecular dynamics (MD) simulations were performed prior to QM/MM calculations. Details of these are provided in the supporting information (SI). The protocols used are similar to those used previously in QM/MM modeling of several CYPs.[9,12,13,38]

The structures from MD simulations were screened before selection as starting models for QM/MM calculations. The selection criteria used in the screening ensured that mexiletine was in a 'reactive' conformation within the active site, with respect to N-hydroxylation, thus giving the most representative reaction barriers. This type of conformational screening has been applied in previous work for the modeling of other P450-catalysed oxidation reactions.[12,39] Structures were selected such that the O-H interatomic distance was less than 3

Å and the Fe-O-H angle was between 110 and 130°, where O and H are the ferryl oxygen of Cpd I and either one of the amine protons of mexiletine, respectively. In the previous small model DFT studies of N-hydroxylation,[33,34] the barriers to N-oxidation and H-abstraction were calculated relative to a common starting structure: That in which a hydrogen bond is present between the Cpd I oxygen and an amine proton, and corresponds to the energy minimum for the reactant complex. In the present study, direct N-oxidation profiles and H-abstraction/rebound profiles were calculated using the same starting structures from MD.

QM/MM calculations were performed using the B3LYP functional[40–43] for the QM region, with an empirical correction for dispersion;[44] inclusion of dispersion effects has been shown to improve DFT modeling of P450-catalysed reactions.[38,45] The LACVP basis set[46] was used for iron and the 6-31G(d) basis set[47] for all other QM atoms (denoted herein as BSI). The CHARMM27 force field[48] was used to describe the MM region. The MM calculations were carried out with Tinker,[49] and the QM calculations with Jaguar.[50] The coupling between the QM and MM calculations and the QM/MM minimization was performed with QoMMMa.[51] Additional single point energy calculations were carried out on the B3LYP-D:6-31G(d)/CHARMM27 optimized geometries for the starting materials, transition states, intermediates and products, using the LACV3P basis set for iron and 6-311++G(d,p) for all other atoms (BSII).

The QM region consisted of 64 atoms: mexiletine, a truncated heme group and a thiolate to represent the Fe-bound cysteine residue. The rest of the atoms in the system were included in the MM region. Hydrogen 'link' atoms were used to cap all of the C-C bonds at the QM-MM boundary.[52] Charges of MM atoms at the QM/MM boundary were set to zero, to avoid any unphysical effects due to interactions with the link atoms.[53]

The nine structures selected from the MD trajectories were QM/MM energy minimized for both the quartet and doublet spin states of Compound I. Reaction pathways were modeled using an adiabatic mapping procedure.[12,39] For the direct N-oxidation reaction, a series of QM/MM energy minimizations was performed with the N-O distance restrained sequen-

7

tially to values between 3 Å and 1.4 Å, varied at intervals of 0.2 Å (0.1 Å and 0.05 Å around the transition state). For the H-abstraction reaction, the same procedure was used for the O-H distance between 2.2 Å and 1 Å. The structure corresponding to the intermediate for H-abstraction was QM/MM minimized without reaction coordinate restraints and subsequently used as the starting geometry for calculating the rebound step. In this step the N-O distance was varied between 2.7 Å (corresponding to the radical intermediate) to 1.4 Å (the product). The product geometry was subsequently energy-minimized without reaction coordinate constraints. Absolute energies of all stationary points are provided in the SI.

In addition to the individual barriers given below, an overall barrier was calculated by a Boltzmann-weighted averaging procedure of the calculated barriers, as detailed in previous work.[39] This averaging scheme compensates for the relatively small amount of conformational sampling in an approximate manner, as it places higher importance on the lower energy barriers, which are likely to be more representative of the true reactivity of the enzyme. For multi-step reactions, barriers were calculated for all steps relative to the energy of the reactant complex (RC).

Single-point calculations were also performed on the stationary points for selected pathways using the BP86[54,55] and BHandHLYP[42,43,46,56] functionals. The energies calculated using these functionals are provided in the SI. The absolute values of the calculated energy barriers were found to differ depending on the choice of functional, however, the qualitative analysis of the barriers is unaffected.

Results and discussion

In order to obtain suitable starting geometries for the QM/MM calculations, MD simulations were performed from four different docked poses of mexiletine in CYP1A2. In total, over 80 ns of MD data were obtained, yielding over 16,000 structural 'snapshots' to use as potential starting geometries. These snapshots exhibited variation in the orientation of mexiletine

within the CYP1A2 active site, and different binding modes of mexiletine were observed. During some sections of the MD simulations, the substrate rotated around such that the ring fragment was pointing towards the active site. This is consistent with the formation of multiple metabolites of mexiletine by CYP1A2, as shown in Scheme 1. However, in such positions, the other oxidation sites were too far away (> 5 Å) from the Cpd I oxygen for reaction to occur (for more details see SI). As our aim here is to study the mechanism of N-hydroxylation, screening of the MD simulations for suitable reactive starting geometries for QM/MM calculations was required, as described above.

The structures of the reactive poses of mexiletine in the active site of CYP1A2 show that several residues are involved in the binding of mexiletine (Figure 1). These interactions include a pi-stacking interaction to Phe226, a hydrogen-bond to the Cpd I oxygen and a hydrogen bond to Thr124 via a bridging water molecule. The importance of bridging water molecules and their changing presence in the active site has been noted previously in other computational studies of CYP reactivity.[57,58] The number of water molecules in the active site varies between simulations and hence the latter interaction is not observed during all of the simulations. Some frames were observed where the amine proton that is otherwise hydrogen-bonded to Thr124 forms a hydrogen bond to the ether oxygen of mexiletine. The hydrogen bond between the amine group of mexiletine and Cpd I ferryl oxygen, as well as the pi-stacking interaction to Phe226, are maintained. Many more (> 5) water molecules were observed in the active site cavity during periods of some simulations. When this occurs, mexiletine is prevented from approaching Cpd I for reaction.

Only three of the four MD simulations yielded suitable starting structures for modeling N-hydroxylation. These were propagated from three different docking poses (details in the SI), each of which contained a different binding conformation of mexiletine in the active site (referred to herein as A, B and C). QM/MM (B3LYP-D/CHARMM27) optimized reactant complexes, derived from each of these simulations (A, B and C) are displayed in Figure 2.

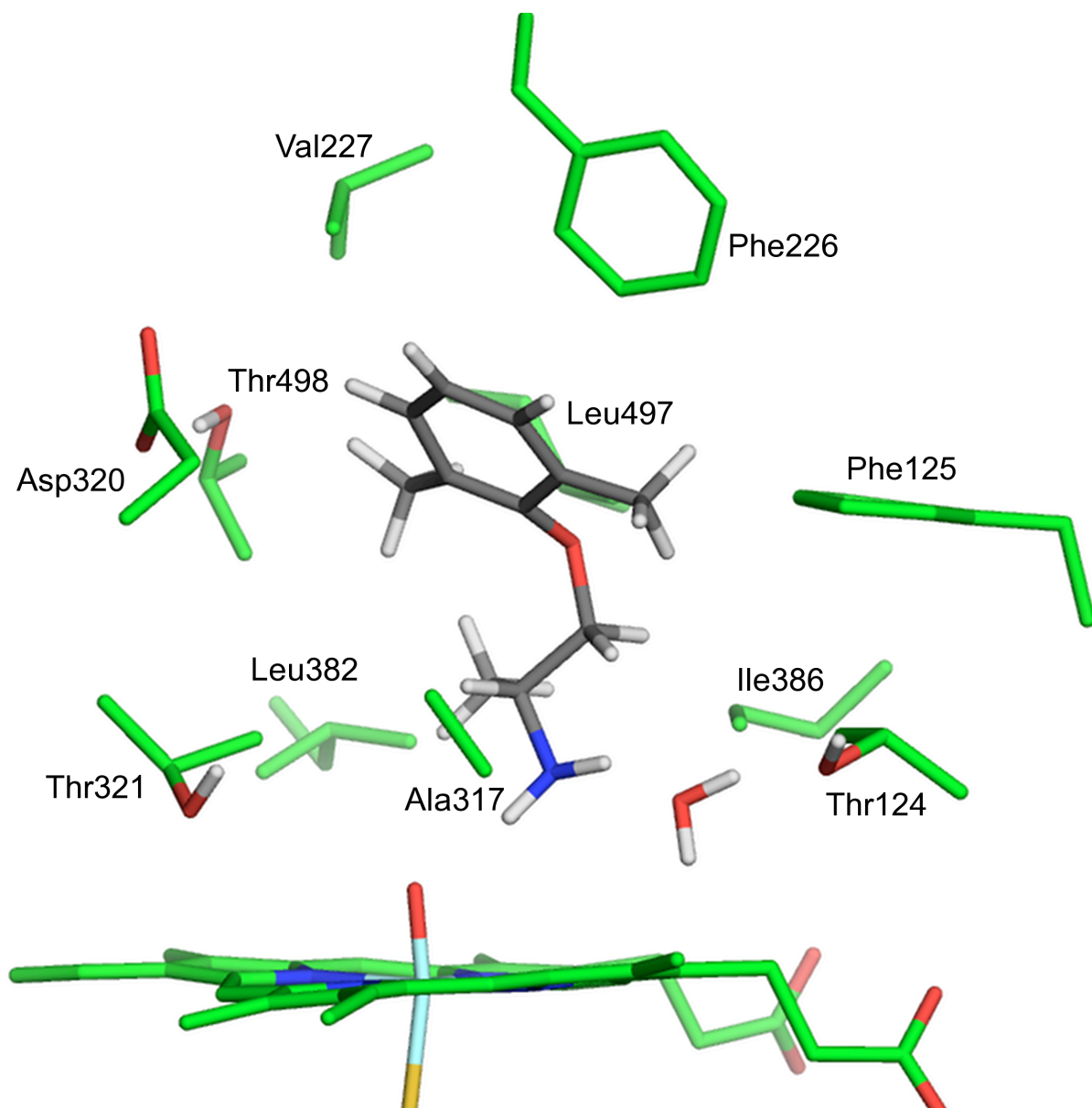Nine QM/MM energy barriers were obtained for the H-abstraction and rebound mech-

Figure 1: Starting structure for H-abstraction profile B-2. This structure was taken from frame 577 of MD simulation 2 of docking pose B. The carbon atoms of mexiletine are displayed in gray.
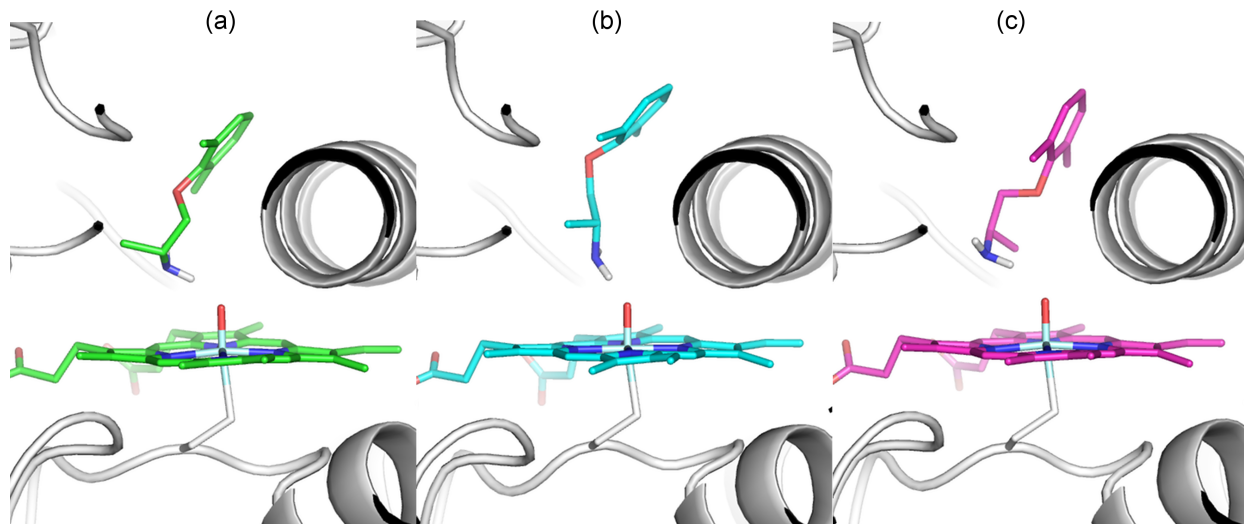
Figure 2: QM/MM (B3LYP-D/CHARMM27) optimized reactant complex (RC) structures for the (a) A-1, (b) B-1 and (c) C-1 reaction profiles.

anism steps in the quartet and doublet spin states. The barriers calculated with BSII are provided in Table 1. Both steps in the mechanism show a wide range of values for the barrier height, but the barrier to the rebound step is generally higher than that for the H-abstraction step; the H-abstraction barriers vary from 6.9 to 17.8 kcal/mol, while the rebound barriers range from 14.3 to 33.8 kcal/mol. The highest H-abstraction barriers are observed for the models where the H-bond between one of the amine protons and Thr124 via a bridging water molecule is not present (A-1, A-3 and C-1). The doublet and quartet barriers tend to be similar for the hydrogen abstraction step, which is consistent with the small model DFT studies of propan-2-amine hydroxylation,[33,34] and also with QM and QM/MM studies of C-H abstraction from alkanes.[59] The Boltzmann-weighted average barrier for the H-abstraction step is 8.1 kcal/mol and is accessible to both the doublet and quartet spin states of Cpd I. This barrier does not include a zero point energy (ZPE) correction; based on values calculated in the small model studies,[33,34] we expect this correction to be in the region of ~ 3 kcal/mol. This would result in a barrier of around 5.1 kcal/mol for the H-abstraction step. The free energy barrier would be somewhat higher, because of activation entropy (see below), but it is expected that this would be of similar magnitude to that of the competing mechanism. The

rebound step has a Boltzmann-weighted average barrier of 15.0 kcal/mol, and is favored on the doublet spin surface. A ZPE correction of 1.7 kcal/mol is estimated, based on previous work,[34] bringing the barrier down to approximately 13.3 kcal/mol.

Table 1: QM/MM barriers [in kcal/mol] for H-abstraction ($\Delta E^{\ddagger}_{HAB}$) and rebound ($\Delta E^{\ddagger}_{REB}$) in the doublet (D) and quartet (Q) spin states (calculated with BSII). The profile labels A, B and C denote the three different docked poses of mexiletine to the crystal structure that were used as initial coordinates for molecular dynamics simulations (see SI for further information).

Profile	$\Delta E^{\ddagger}_{HAB}$		$\Delta E^{\ddagger}_{REB}$	
	D	Q	D	Q
A-1	17.4	15.4	14.3	18.4
A-2	14.4	14.9	18.5	21.3
A-3	17.8	17.7	22.8	33.8
B-1	14.2	15.0	16.8	26.3
B-2	6.9	7.2	16.0	20.1
B-3	8.6	14.9	14.4	27.5
B-4	10.3	14.7	15.5	26.0
B-5	8.3	8.3	21.7	25.5
C-1	15.9	14.6	14.4	14.9
$\Delta E^{\ddagger}_{Ave}$	12.4	13.6	17.2	23.8
$\Delta E^{\ddagger}_{B-Ave}$	8.1	8.4	15.0	16.2

The optimized geometries for the H-abstraction step are similar between the doublet and quartet spin states for a given pathway. The QM geometries of the key intermediates for the B-1 pathway are provided as representative examples in the SI. The transition state to H-abstraction was observed at the same position on the potential energy surface for all starting models (corresponding to an O−H distance of ∼ 1.2 Å). During the rebound step, not all of the pathways went to the hydroxamine product (**2**, Figure 3(a)): In the case of the A-1, A-2, A-3, B-2 (all doublet+quartet) and B-3 (doublet only) pathways the abstracted hydrogen spontaneously returns to the mexiletine nitrogen before the N−O bond formation takes place, yielding the N-oxide product (Figure 3(b)). Hence, in this case, the same intermediate is formed as that formed during the N-oxidation process. This alternative process results in two separate barriers on the potential energy surface, the highest one (the

return of the proton) is the one reported in Table 1. Large differences in barrier are observed between the two spin surfaces for the rebound step. The doublet barriers are considerably lower than those calculated for the quartet state, in some cases by more than 10 kcal/mol. The preference for the doublet spin state during the rebound step is consistent with previous work.[33,34]

The combined results for the H-abstraction/rebound mechanism show that this mechanism favors the doublet spin surface and that the rate-limiting step is the rebound process. The Boltzmann-weighted average barrier for this mechanism is approximately 13.3 kcal/mol. Whilst some of the details of this mechanism are similar to those of the small model DFT study of propan-2-amine oxidation,[33,34] the present study shows that the rebound step is rate-limiting, whereas in the most recent DFT study[34] it was found that the H-abstraction step was likely to be rate-limiting. However, the difference in energy barriers between the two steps for propan-2-amine is small (less than 1 kcal/mol on the doublet spin surface), and the overall energy barriers to the rebound step are very close in magnitude (within 1 kcal/mol). As our QM/MM calculations include specific interactions with the protein/solvent environment, including the steric effects of the surrounding residues and the H-bonding interaction with the water molecule bound to Thr124, this represents a more detailed model of the reaction taking place. Furthermore, the previous work[34] found that for other amine substrates, the rebound steps were indeed rate-limiting.

Nine QM/MM reaction profiles were calculated for the direct N-oxidation mechanism, from different initial starting geometries. The barriers are displayed in Table 2. As with the H-abstraction/rebound mechanism, a wide range of barriers is observed. The BSII calculated barriers range between 7.7 and 33.4 kcal/mol, with a Boltzmann-weighted average value of 9.0 kcal/mol on the doublet spin surface. The $N-O$ bond formation step involves the transfer of two electrons from the substrate to Cpd I. The transfer of the second electron requires significantly more energy in the case of the quartet state, compared to the doublet. The transition state for the doublet N-O bond formation step is earlier than that of the quartet

(see SI), and corresponds to inversion at the nitrogen atom, rather than the electron transfer step, which appears as a shoulder on the peak corresponding to the inversion step. This finding is in good agreement with the previous small model study of propan-2-amine.[33]

Table 2: QM/MM barriers [in kcal/mol] for N-oxidation ($\Delta E^{\ddagger}_{NOX}$) in the doublet (D) and quartet (Q) spin states (calculated with BSII). The profile labels A, B and C denote the three different docked poses of mexiletine to the crystal structure that were used as initial coordinates for molecular dynamics simulations (see SI for further information).

Profile	$\Delta E^{\ddagger}_{NOX}$	
	D	Q
A-1	7.7	21.6
A-2	11.1	23.0
A-3	11.0	30.3
B-1	11.9	18.8
B-2	19.5	17.5
B-3	24.0	30.8
B-4	12.8	28.4
B-5	20.2	21.5
C-1	22.7	33.4
$\Delta E^{\ddagger}_{Ave}$	15.7	25.0
$\Delta E^{\ddagger}_{B-Ave}$	9.0	18.7

The Boltzmann-weighted average values of the BSII calculated reaction profiles for both oxidation mechanisms are shown in Figure 4. The relative energies of all points on the doublet potential energy surface are lower than the corresponding points on the quartet spin surface. It is therefore likely that the doublet spin state is dominant for the N-hydroxylation reaction of mexiletine as catalysed by CYP1A2. Previous calculations performed on the N-hydroxylation of primary amines[33] have found this to be the case for the N-oxidation reaction, but similar barriers for the doublet and quartet spin states were reported for the H-abstraction and rebound mechanism. Here we observed similar barriers for H-abstraction between the doublet and quartet spin states, however, the doublet rebound barriers are consistently lower than their quartet counterparts. The N-oxidation reaction is unfavorable on the quartet spin surface compared to the doublet because the two electrons donated by
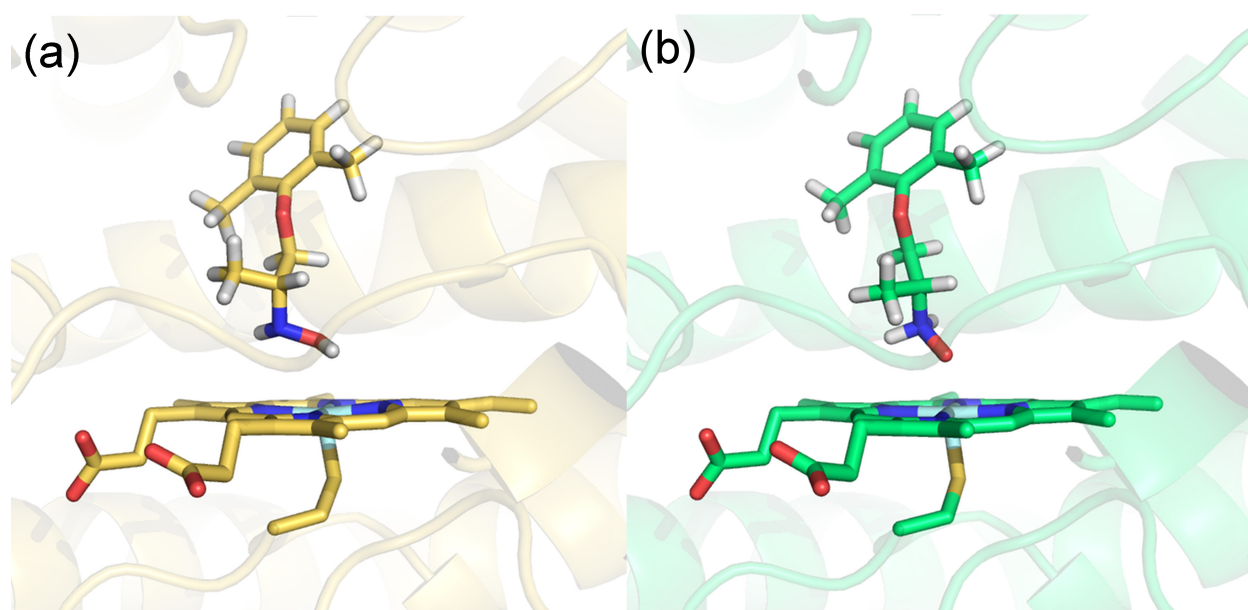
Figure 3: QM/MM (B3LYP-D/CHARMM27) optimized structures of (a) product of H-abstraction followed by rebound, P_{HABS}; (b) product of direct N-oxidation, P_{NOX}.

the substrate are of opposite spin, and for them to be accepted by the quartet spin state of Cpd I requires that one of these electrons goes into a high energy unoccupied 3d orbital. In contrast, this promotion is not required for the doublet spin state of Cpd I, as the two electrons from the substrate can be accommodated by the singly occupied a_{2u} and FeO π^* orbitals, which contain electrons of opposite spin.[60–62]

The experimentally derived free energy barrier for the N-hydroxylation of mexiletine in CYP1A2 (at 310 K), derived using transition state theory[63,64] from a reported experimentally measured turnover number of 110 pmoles/nmole P450/min,[26] is 21.3 kcal/mol. This is significantly higher than our Boltzmann-weighted average barriers for either mechanism (and also the case if simple averaging of the energy barriers is used). There are several possible reasons for this difference. Firstly, the calculated barriers quoted here are not free energy barriers (unlike the experimental value) and therefore do not include entropic effects, which are expected to raise the barrier by ~ 3 kcal/mol, based on calculations of similar reactions.[65,66] This should always be considered when comparing potential energy barriers with apparent free energy barriers derived from experimental kinetic measurements. Also there can be additional free energy penalties for conformational changes and reactions may proceed via minor, higher energy binding modes or conformations.[12] Secondly, it is not established which step in the catalytic cycle is rate-determining for the N-hydroxylation reaction; previous studies on a number of different systems have shown a variety of steps to be rate-limiting for CYPs, including the second electron transfer step, the C−H bond breaking step for aliphatic oxidation, and an unidentified step between product formation and release.[67] For this reason, the N-hydroxylation reaction barrier may not necessarily be the same as the reaction barrier for the whole catalytic cycle. Thirdly, DFT calculated barriers are sometimes (but not always) too low by several kcal/mol.[68] Further discrepancies can be due to artefacts associated with QM/MM methods.[69] Finally, contributions from tunnelling are also often an important consideration when modeling H-atom transfer.[70]

A further important factor to consider is the contribution of the binding of the substrate
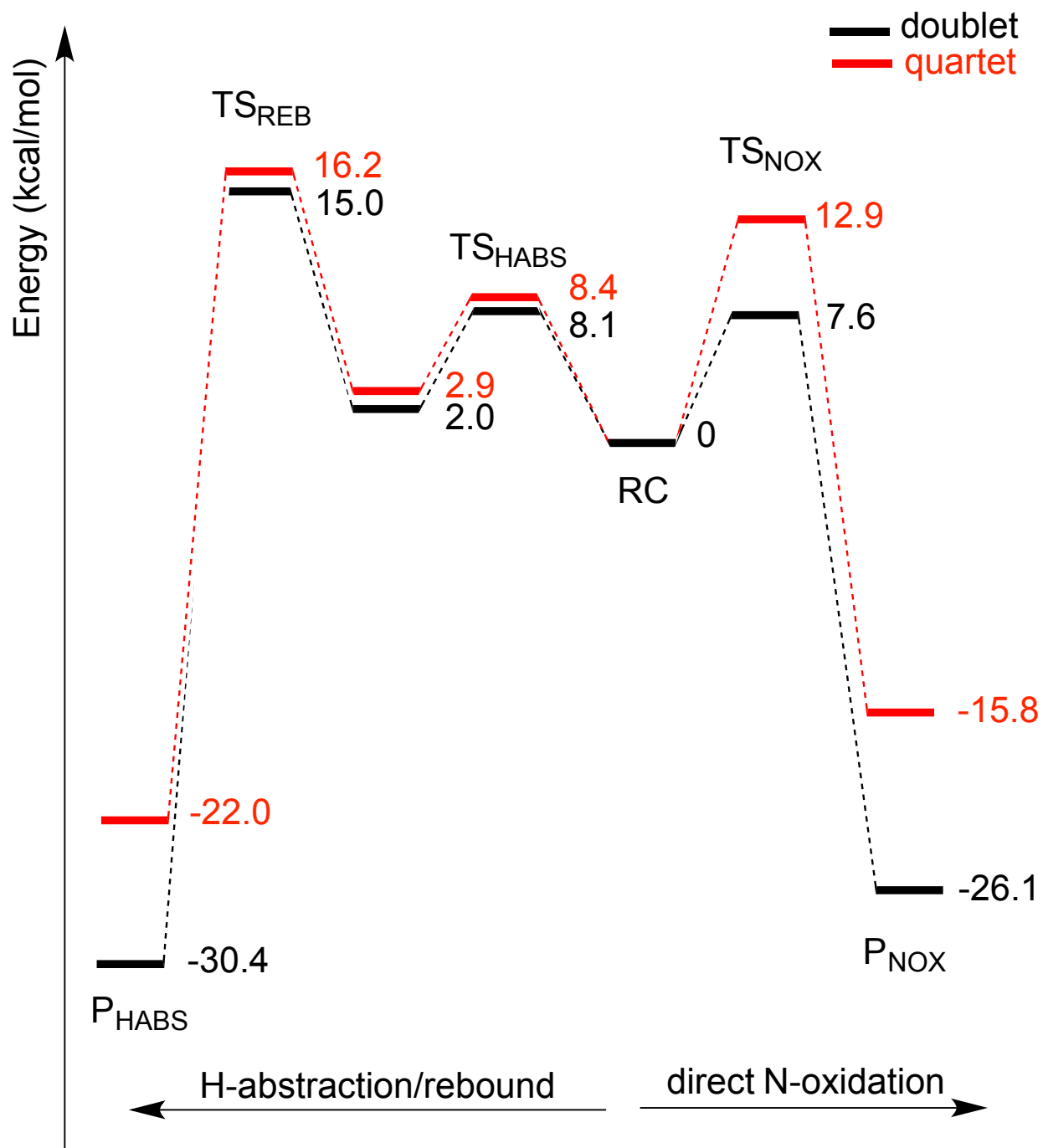
Figure 4: Reaction profiles for direct N-oxidation and H-abstraction/rebound mechanisms. Energies of all species [in kcal/mol] are Boltzmann-weighted average values calculated at the B3LYP-D-6-311++G(d,p)/CHARMM27 level of QM/MM theory.

into a reactive position to the overall barrier. The averaging of barriers using a Boltzmann weighting will not take into account the fact that different substrate conformations may be more of less prevalent, for example it is not known to what extent conformations A, B and C differ in binding free energy. Hence the true overall barrier will reflect both the barrier to reaction and the free energy of binding of the substrate in the respective reactive orientation. We have found this to be the case previously for oxidation of diclofenac in CYP2C9, where a higher barrier process is favored over a lower barrier process due to the Michaelis complex having a more favorable binding free energy in the former.[12] However, in the present case, the substrate binding conformations are very similar to each other. Therefore, it is reasonable here to make comparisons based on energy barriers alone.

Conclusions

In the current study, the mechanism for the oxidation of primary amines has been investigated using a large and detailed enzyme-substrate model, in which the effects of the surrounding enzyme environment are included explicitly. Two mechanisms have been proposed[31] for the N-hydroxylation of mexiletine, catalysed by CYP1A2: direct N-oxidation, and hydrogen abstraction followed by rebound. The two mechanisms were modeled for the doublet and quartet spin states of Cpd I using QM/MM, and the direct nitrogen oxidation mechanism was found to be more energetically favorable. These results differ somewhat from a recent small model DFT study where simpler primary amines were used as substrates.[34] However, in the previous study, the relative difference in barrier between the two mechanisms varied depending on the substrate in question. It is therefore possible that the two mechanisms compete in nature, with N-oxidation being favored for this particular substrate. For both mechanisms, the reaction barriers were found to be lower in energy for the doublet spin state of Cpd I, than for the quartet spin state, with a more pronounced effect observed for the N-oxidation mechanism.

A wide range of values is observed here for the reaction barriers for each mechanism and spin state. This is due to the use of a variety different starting geometries, despite pre-screening of molecular dynamics (MD) snapshots. A Boltzmann-weighted averaging procedure was used to ensure that the lowest, and therefore most relevant values are given a greater weighting. It is well accepted that in order to obtain reliable results, an adequately sized ensemble of starting geometries must be used.[39] Ideally, many more reaction profiles would have been calculated for each mechanism and spin state, however this is not practical due to the high computational cost of running such QM/MM calculations. This makes the pre-screening of snapshots and the selection of suitable geometric criteria of great importance.[39,71]

A series of MD simulations was carried out in order to find reactive conformations of mexiletine within the active site. The presence of a single water molecule was found to play a large role on keeping mexiletine in a reactive position within the active site. When significantly more water molecules (> 5) were present, mexiletine was displaced from a reactive position. A bridging water molecule was observed between the mexiletine and Thr124, orienting the mexiletine in a reactive conformation throughout the simulation. The water molecule is not a prerequisite for mexiletine binding, however, in simulations where a single water molecule was present, mexiletine remained in a reactive conformation for a larger proportion of the simulation than when the water molecule was absent. A pi-stacking interaction was observed between the substrate and Phe226, in all of the transition state structures, whether or not a water molecule was present.

Increased knowledge of cytochrome P450 activity and mechanisms gained through studies such as this should be useful in improving drug reactivity and metabolism prediction, as well as increasing their applications in biocatalysis.[9,12,14]

Dedication

This manuscript is dedicated to Dr. Patrik Rydberg, who actively contributed to this project but sadly passed away prior to the publication of this work.

Funding Information

Acknowledgement

Supporting Information Available

Details of intial structure preparation and MD simulations; MM parameters for mexiletine; selected interatomic distances calculated during MD simulations; QM/MM energies of all species calculated with BSI and BSII; QM/MM energies of selected species calculated with other DFT functionals; coordinates of QM region of stationary points for profile B1.

This material is available free of charge via the Internet at `http://pubs.acs.org/`.

Abbreviations

QM/MM - Quantum Mechanics/Molecular Mechanics; CYP - cytochrome P450; MD - molecular dynamics; DFT - density functional theory; ZPE - zero point energy.

References

(1) Anzenbacher, P., and Anzenbacherová, E. (2001) Cytochromes P450 and metabolism of xenobiotics. *Cell. Mol. Life Sci. 58*, 737–747.

(2) Guengerich, F. P. In *The Ubiquitous Roles of Cytochrome P450 Proteins*; Sigel, A., Sigel, H., and Sigel, R. K. O., Eds.; Metal Ions in Life Sciences; John Wiley & Sons, Ltd: Chichester, 2007; Vol. 3; pp 561–589.

(3) Ortiz de Montellano, P. R. (1995) The 1994 Bernard B. Brodie Award Lecture. Structure, mechanism, and inhibition of cytochrome P450. *Drug Metab. Dispos. 23*, 1181–1187.

(4) Slaughter, R., and Edwards, D. (1995) Recent advances: the cytochrome P450 enzymes. *Ann. Pharmacother. 29*, 619–624.

(5) Pirmohamed, M., and Park, B. (2003) Cytochrome P450 enzyme polymorphisms and adverse drug reactions. *Toxicology 192*, 23 – 32.

(6) Rydberg, P., Gloriam, D. E., Zaretzki, J., Breneman, C., and Olsen, L. (2010) SMART-Cyp: A 2D Method for Prediction of Cytochrome P450-Mediated Drug Metabolism. *ACS Med. Chem. Lett. 1*, 96–100.

(7) Rittle, J., and Green, M. T. (2010) Cytochrome P450 Compound I: Capture, Characterization, and C-H Bond Activation Kinetics. *Science 330*, 933–937.

(8) Rittle, J., Younker, J. M., and Green, M. T. (2010) Cytochrome P450: The Active Oxidant and Its Spectrum. *Inorg. Chem. 49*, 3610–3617.

(9) Lonsdale, R., Harvey, J. N., and Mulholland, A. J. In *Iron-Containing Enzymes: Versatile Catalysts of Hydroxylation Reactions in Nature*; de Visser, S. P., and Kumar, D., Eds.; RSC Publishing, 2011; Chapter 11, pp 366–399.

(10) Shaik, S., Cohen, S., Wang, Y., Chen, H., Kumar, D., and Thiel, W. (2009) P450 Enzymes: Their Structure, Reactivity, and Selectivity—Modeled by QM/MM Calculations. *Chem. Rev. 110*, 949–1017.

(11) Li, D., Huang, X., Han, K., and Zhan, C.-G. (2011) Catalytic Mechanism of Cytochrome P450 for 5'-Hydroxylation of Nicotine: Fundamental Reaction Pathways and Stereoselectivity. *J. Am. Chem. Soc. 133*, 7416–7427.

(12) Lonsdale, R., Houghton, K. T., Żurek, J., Bathelt, C. M., Foloppe, N., de Groot, M. J., Harvey, J. N., and Mulholland, A. J. (2013) Quantum Mechanics/Molecular Mechanics Modeling of Regioselectivity of Drug Metabolism in Cytochrome P450 2C9. *J. Am. Chem. Soc. 135*, 8001–8015.

(13) Oláh, J., Mulholland, A. J., and Harvey, J. N. (2011) Understanding the determinants of selectivity in drug metabolism through modeling of dextromethorphan oxidation by cytochrome P450. *Proc. Nat. Acad. Sci. U.S.A. 108*, 6050–6055.

(14) Lonsdale, R., and Mulholland, A. J. (2014) QM/MM Modelling of Drug-Metabolizing Enzymes. *Curr. Top. Med. Chem. 14*, 1339–1347.

(15) Lonsdale, R., Rouse, S. L., Sansom, M. S. P., and Mulholland, A. J. (2014) A Multiscale Approach to Modelling Drug Metabolism by Membrane-Bound Cytochrome P450 Enzymes. *PLoS Comput. Biol. 10*, e1003714.

(16) Ji, L., Faponle, A. S., Quesne, M. G., Sainna, M. A., Zhang, J., Franke, A., Kumar, D., vanEldik, R., Liu, W., and deVisser, S. P. (2015) Drug Metabolism by Cytochrome P450 Enzymes: What Distinguishes the Pathways Leading to Substrate Hydroxylation Over Desaturation? *Chem.- Eur. J. 21*, 9083–9092.

(17) Lewis, D. F. V., Lake, B. G., Dickins, M., Ueng, Y.-F., and Goldfarb, P. S. (2003) Homology modelling of human CYP1A2 based on the CYP2C5 crystallographic template structure. *Xenobiotica 33*, 239–254.

(18) Zhou, S.-F., Yang, L.-P., Zhou, Z.-W., Liu, Y.-H., and Chan, E. (2009) Insights into the Substrate Specificity, Inhibitors, Regulation, and Polymorphisms and the Clinical Impact of Human Cytochrome P450 1A2. *AAPS J. 11*, 481–494.

(19) Lee, A. J., Cai, M. X., Thomas, P. E., Conney, A. H., and Zhu, B. T. (2003) Characterization of the Oxidative Metabolites of 17β-Estradiol and Estrone Formed by 15 Selectively Expressed Human Cytochrome P450 Isoforms. *Endocrinology 144*, 3382–3398.

(20) Campbell, R. W. (1987) Mexiletine. *N. Engl. J. Med. 316*, 29–34.

(21) Moak, J. P., Smith, R. T., and Garson, J. A. (1987) Mexiletine: An effective antiarrhythmic drug for treatment of ventricular arrhythmias in congenital heart disease. *J. Am. Coll. Cardiol. 10*, 824–829.

(22) Turgeon, J., Uprichard, A. C. G., Bélanger, P. M., Harron, D. W. G., and Grech-Bélanger, O. (1991) Resolution and Electrophysiological Effects of Mexiletine Enantiomers. *J. Pharm. Pharmacol. 43*, 630–635.

(23) Campbell, N. P., Kelly, J. G., Adgey, A. A., and Shanks, R. G. (1978) The clinical pharmacology of mexiletine. *Br. J. Clin. Pharmacol. 6*, 103–108.

(24) Campbell, R. W. F., Dolder, M. A., Prescott, L. F., Talbot, R. G., Murray, A., and Julian, D. G. (1975) Comparison of Procainamide and Mexiletine in Prevention of Ventricular Arrhythmias After Acute Myocardial Infarction. *Lancet 305*, 1257–1260.

(25) Broly, F., Libersa, C., and Lhermitte, M. (1990) Mexiletine metabolism in vitro by human liver. *Drug Metab. Dispos. 18*, 362–368.

(26) Labbè, L., Abolfathi, Z., Lessard, È., Pakdel, H., Beaune, P., and Turgeon, J. (2003) Role of specific cytochrome P450 enzymes in the N-oxidation of the antiarrhythmic agent mexiletine. *Xenobiotica 33*, 13–25.

(27) Nakajima, M., Kobayashi, K., Shimada, N., Tokudome, S., Yamamoto, T., and Kuroiwa, Y. (1998) Involvement of CYP1A2 in mexiletine metabolism. *Br. J. Clin. Pharmacol. 46*, 55–62.

(28) Turgeon, J., Fiset, C., Giguère, R., Gilbert, M., Moerike, K., Rouleau, J. R., Kroemer, H. K., Eichelbaum, M., Grech-Bélanger, O., and Bélanger, P. M. (1991) Influence of debrisoquine phenotype and of quinidine on mexiletine disposition in man. *J. Pharmacol. Exp. Ther. 259*, 789–798.

(29) de Groot, M. J., Bijloo, G. J., Martens, B. J., van Acker, F. A. A., and Vermeulen, N. P. E. (1997) A Refined Substrate Model for Human Cytochrome P450 2D6. *Chem. Res. Toxicol. 10*, 41–48.

(30) Evelo, C. T., Spooren, A. A., Bisschops, R. A., Baars, L. G., and Neis, J. M. (1998) Two Mechanisms for Toxic Effects of Hydroxylamines in Human Erythrocytes: Involvement of Free Radicals and Risk of Potentiation. *Blood Cells, Mol. Dis. 24*, 280–295.

(31) Nishida, C. R., Knudsen, G., Straub, W., and Ortiz de Montellano, P. R. (2002) Electron Supply and Catalytic Oxidation of Nitrogen by Cytochrome P450 and Nitric Oxide Synthase. *Drug Metab. Rev. 34*, 479–501.

(32) Groves, J. T., and McClusky, G. A. (1976) Aliphatic hydroxylation via oxygen rebound. Oxygen transfer catalyzed by iron. *J. Am. Chem. Soc. 98*, 859–861.

(33) Rydberg, P., and Olsen, L. (2011) Do Two Different Reaction Mechanisms Contribute to the Hydroxylation of Primary Amines by Cytochrome P450? *J. Chem. Theory Comput. 7*, 3399–3404.

(34) Seger, S. T., Rydberg, P., and Olsen, L. (2015) Mechanism of the N-Hydroxylation of Primary and Secondary Amines by Cytochrome P450. *Chem. Res. Toxicol. 28*, 597–603.

(35) Ji, L., and Schüürmann, G. (2013) Model and Mechanism: N-Hydroxylation of Primary Aromatic Amines by Cytochrome P450. *Angew. Chem., Int. Ed. 52*, 744–748.

(36) Rydberg, P., Jørgensen, M. S., Jacobsen, T. A., Jacobsen, A.-M., Madsen, K. G., and Olsen, L. (2013) Nitrogen Inversion Barriers Affect the N-Oxidation of Tertiary Alkylamines by Cytochromes P450. *Angew. Chem. Int. Ed. 52*, 993–997.

(37) Sansen, S., Yano, J. K., Reynald, R. L., Schoch, G. A., Griffin, K. J., Stout, C. D., and Johnson, E. F. (2007) Adaptations for the Oxidation of Polycyclic Aromatic Hydrocarbons Exhibited by the Structure of Human P450 1A2. *J. Biol.Chem. 282*, 14348–14355.

(38) Lonsdale, R., Harvey, J. N., and Mulholland, A. J. (2010) Inclusion of Dispersion Effects Significantly Improves Accuracy of Calculated Reaction Barriers for Cytochrome P450 Catalyzed Reactions. *J. Phys. Chem. Lett. 1*, 3232–3237.

(39) Lonsdale, R., Harvey, J. N., and Mulholland, A. J. (2010) Compound I Reactivity Defines Alkene Oxidation Selectivity in Cytochrome P450cam. *J. Phys. Chem. B 114*, 1156–1162.

(40) Vosko, S. H., Wilk, L., and Nusair, M. (1980) Accurate spin-dependent electron liquid correlation energies for local spin density calculations: a critical analysis. *Can. J. Phys. 58*, 1200–1211.

(41) Kameo, H., Ishii, S., and Nakazawa, H. (2012) Synthesis of iridium complexes bearing {o-(Ph_2P)C_6H_4)}$_3$E type (E = Si, Ge, and Sn) ligand and evaluation of electron donating ability of group 14 elements E. *Dalton Trans. 41*, 8290–8296.

(42) Becke, A. D. (1993) Density-functional thermochemistry. III. The role of exact exchange. *J. Chem. Phys. 98*, 5648–5652.

(43) Stephens, P. J., Devlin, F. J., Chabalowski, C. F., and Frisch, M. J. (1994) Ab Initio

Calculation of Vibrational Absorption and Circular Dichroism Spectra Using Density Functional Force Fields. *J. Phys. Chem. 98*, 11623–11627.

(44) Grimme, S. (2006) Semiempirical GGA-type density functional constructed with a long-range dispersion correction. *J. Comput. Chem. 27*, 1787–1799.

(45) Lonsdale, R., Harvey, J. N., and Mulholland, A. J. (2012) Effects of Dispersion in Density Functional Based QM/MM Calculations on Cytochrome P450 Catalyzed Reactions. *J. Chem. Theory Comput. 8*, 4637–4645.

(46) Hay, P. J., and Wadt, W. R. (1985) Ab initio effective core potentials for molecular calculations. Potentials for K to Au including the outermost core orbitals. *J. Chem. Phys. 82*, 299–310.

(47) Rassolov, V. A., Ratner, M. A., Pople, J. A., Redfern, P. C., and Curtiss, L. A. (2001) 6-31G* basis set for third-row atoms. *J. Comput. Chem. 22*, 976–984.

(48) MacKerell, A. D. et al. (1998) All-Atom Empirical Potential for Molecular Modeling and Dynamics Studies of Proteins. *J. Phys. Chem. B 102*, 3586–3616.

(49) Ponder, J. W. TINKER: Software Tools for Molecular Design. 2003.

(50) Jaguar, 5th Ed., Schrödinger, L.L.C: Portland, OR. 2003.

(51) Harvey, J. N. (2004) Spin-forbidden CO ligand recombination in myoglobin. *Faraday Discuss. 127*, 165–177.

(52) Singh, U. C., and Kollman, P. A. (1986) A combined ab initio quantum mechanical and molecular mechanical method for carrying out simulations on complex molecular systems: Applications to the $CH_3Cl + Cl^-$ exchange reaction and gas phase protonation of polyethers. *J. Comput. Chem. 7*, 718–730.

(53) König, P. H., Hoffmann, M., Frauenheim, T., and Cui, Q. (2005) A Critical Evaluation of Different QM/MM Frontier Treatments with SCC-DFTB as the QM Method. *J. Phys. Chem. B 109*, 9082–9095.

(54) Becke, A. D. (1988) Density-functional exchange-energy approximation with correct asymptotic-behavior. *Phys. Rev. A 38*, 3098–3100.

(55) Perdew, J. P. (1986) Density-functional approximation for the correlation energy of the inhomogeneous electron gas. *Phys. Rev. B 33*, 8822–8824.

(56) Becke, A. D. (1997) Density-functional thermochemistry. V. Systematic optimization of exchange-correlation functionals. *J. Chem. Phys. 107*, 8554–8560.

(57) Bren, U., and Oostenbrink, C. (2012) Cytochrome P450 3A4 Inhibition by Ketoconazole: Tackling the Problem of Ligand Cooperativity Using Molecular Dynamics Simulations and Free-Energy Calculations. *J. Chem. Inf. Model. 52*, 1573–1582.

(58) Bren, U., Fuchs, J. E., and Oostenbrink, C. (2014) Cooperative Binding of Aflatoxin B1 by Cytochrome P450 3A4: A Computational Study. *Chem. Res. Toxicol. 27*, 2136–2147.

(59) Shaik, S., Cohen, S., de Visser, S. P., Sharma, P. K., Kumar, D., Kozuch, S., Ogliaro, F., and Danovich, D. (2004) The "Rebound Controversy": An Overview and Theoretical Modeling of the Rebound Step in C−H Hydroxylation by Cytochrome P450. *Eur. J. Inorg. Chem. 2004*, 207–226.

(60) Ogliaro, F., Cohen, S., de Visser, S. P., and Shaik, S. (2000) Medium Polarization and Hydrogen Bonding Effects on Compound I of Cytochrome P450: What Kind of a Radical Is It Really? *J. Am. Chem. Soc. 122*, 12892–12893.

(61) Rydberg, P., Sigfridsson, E., and Ryde, U. (2004) On the role of the axial ligand in heme proteins: a theoretical study. *J. Biol. Inorg. Chem. 9*, 203–223.

(62) Schöneboom, J. C., Lin, H., Reuter, N., Thiel, W., Cohen, S., Ogliaro, F., and Shaik, S. (2002) The Elusive Oxidant Species of Cytochrome P450 Enzymes: Characterization by Combined Quantum Mechanical/Molecular Mechanical (QM/MM) Calculations. *J. Am. Chem. Soc. 124*, 8142–8151.

(63) Glowacki, D. R., Harvey, J. N., and Mulholland, A. J. (2012) Taking Ockham's razor to enzyme dynamics and catalysis. *Nature Chem. 4*, 169–176.

(64) Truhlar, D. G., Garrett, B. C., and Klippenstein, S. J. (1996) Current Status of Transition-State Theory. *J. Phys. Chem. 100*, 12771–12800.

(65) Claeyssens, F., Harvey, J. N., Manby, F. R., Mata, R. A., Mulholland, A. J., Ranaghan, K. E., Schütz, M., Thiel, S., Thiel, W., and Werner, H.-J. (2006) High-Accuracy Computation of Reaction Barriers in Enzymes. *Angew. Chem. Int. Ed. 45*, 6856–6859.

(66) Senn, H. M., Kästner, J., Breidung, J., and Thiel, W. (2009) Finite-temperature effects in enzymatic reactions - Insights from QM/MM free-energy simulations. *Can. J. Chem. 87*, 1322–1337.

(67) Guengerich, F. P. (2002) Rate-Limiting Steps in Cytochrome P450 Catalysis. *Biol. Chem. 383*, 1553–1564.

(68) Harvey, J. N. (2006) On the accuracy of density functional theory in transition metal chemistry. *Annu. Rep. Prog. Chem., Sect. C: Phys. Chem. 102*, 203–226.

(69) Kaiyawet, N., Lonsdale, R., Rungrotmongkol, T., Mulholland, A. J., and Hannongbua, S. (2015) High-Level QM/MM Calculations Support the Concerted Mechanism for Michael Addition and Covalent Complex Formation in Thymidylate Synthase. *J. Chem. Theory Comput. 11*, 713–722.

(70) Masgrau, L., Roujeinikova, A., Johannissen, L. O., Hothi, P., Basran, J., Ranaghan, K. E., Mulholland, A. J., Sutcliffe, M. J., Scrutton, N. S., and Leys, D. (2006) Atomic Description of an Enzyme Reaction Dominated by Proton Tunneling. *Science 312*, 237–241.

(71) Cooper, A. M., and Kästner, J. (2014) Averaging Techniques for Reaction Barriers in QM/MM Simulations. *ChemPhysChem 15*, 3264–3269.

Graphical TOC Entry

direct N-oxidation

H-abstraction

Mexiletine + CYP1A2